Rev. Roum. Sci. Techn.– Électrotechn. et Énerg.
Vol. **63**, *2*, pp. 151–155, Bucarest, 2018

Dedicated to the memory of Academician Andrei Țugulea

ANALYSIS OF A GRID TIE DUAL ROTOR COUNTER ROTATING WIND SYSTEM

TIBERIU TUDORACHE, VALERIU BOSTAN

Key words: Dual rotor counter rotating wind system, Permanent magnet generators, Finite element, System analysis.

This paper deals with the study of a grid tie small power dual rotor counter rotating wind system. The mechanical energy delivered by the two rotors with fixed-pitch blades is converted into electricity by two permanent magnet synchronous generators operating in parallel, each one being equipped with a maximum power point tracking system. The two machines are designed and analyzed by finite element method implemented into the software package Flux ® and the parameters of each machine are extracted and used in a Matlab/Simulink model that includes the turbines, the generators and all the power electronics blocks required for the grid tie energy conversion system.

1. INTRODUCTION

Wind energy is one of the most exploited renewable energy sources in the world. Wind conversion systems (WCS) provided in 2016 about 10.4 % of the electric energy demand of the European Union [1]. In the same year, the WCS produced in Romania (according to Transelectrica SA data) about 12.16 % of the total consumed electricity.

The common wind turbines have horizontal axis and the rotor is equipped with three blades. The wind kinetic energy is converted into rotational mechanical energy by the wind turbine and then into electricity by synchronous or asynchronous generators [2–7].

The conversion efficiency of a wind turbine can be increased by replacing the classical three-blade rotor with two counter-rotating rotors spinning at different speeds. This solution was analyzed in many papers especially from mechanics and aerodynamics point of view [8–10].

The common electric generators used for the counter-rotating wind systems (CRWS) have two moving parts, an inner one with permanent magnets (PMs) and an outer one (an armature) equipped with three-phase windings system spinning in opposite direction [11]. Such machines have brushes and slip rings, elements that reduce the equipment reliability.

Another possible solution that can be used as electric generator for CRWS is proposed in [12] and consists of an inner PM synchronous generator (PMSG) driven by the high speed turbine (small diameter turbine) which produces electricity to energize the rotor circuit of a bigger outer induction generator (IG) driven by the low speed turbine (large diameter turbine). The presence of the IG operating at small speeds makes this solution less interesting from efficiency point of view.

The electro-mechanical converter used for the CRWS to produce electricity, which is analyzed in this paper, has a special topology, with two coaxially embedded PMSGs for space savings reasons, Fig. 1. The use of PMs on both generators makes them more efficient and reliable since no brushes are used. The design of the machines was carried out using analytical calculation models and the solutions were refined by finite element method (FEM) implemented in Flux ® software package [13]. The generator parameters were estimated by FEM and used further to design the control system of a small power grid tie CRWS, using Matlab-Simulink ® software package.

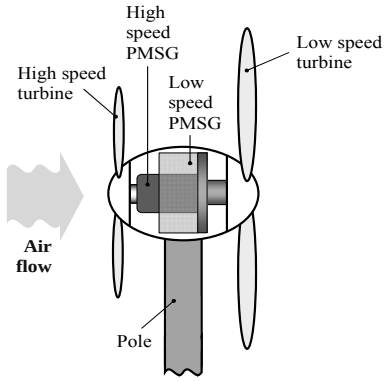

Fig. 1 – Main parts of the studied CRWS.

2. DESIGN OF PMSGS FOR CRWS

The embedded PMSGs dedicated to CRWS were sized using analytical models and the obtained solutions were refined by FEM. The preliminary value of the stator bore diameter D was calculated using the following expression [14]:

$$D = \sqrt[3]{\frac{2p}{\pi\lambda}\frac{60S_i}{n_n C}}, \quad (1)$$

where λ is the machine shape factor, p is the number of pole pairs, S_i is the inner apparent power, n_n is the machine rated speed, and C is the materials utilization coefficient.

The number of turns per phase w_1 was calculated as follows [14]:

$$w_1 = \frac{k_E V_n}{4k_B f_n k_w \Phi}, \quad (2)$$

where k_B is a coefficient depending on the shape of e.m.f., k_E is the ratio between the e.m.f. and terminal voltage, k_w is the winding factor, f_n is the rated frequency and Φ is the magnetic flux per pole.

The FEM analysis of the machines was carried out using the professional software package Flux ® [13]. The 2D computation domain for no-load operation of the machines, the main physical regions and the FE mesh are shown in Fig. 2.

"Politehnica" University of Bucharest, Electrical Engineering Faculty, Bucharest, tiberiu.tudorache@upb.ro

The machines analysis was carried out by solving 2D transient magnetic field problems governed by the following partial differential equation expressed in magnetic vector potential $\boldsymbol{A}$ [13]:

$$\nabla \times \left[\left(\frac{1}{\mu} \right) \nabla \times \boldsymbol{A} - \boldsymbol{H_c} \right] - \boldsymbol{J} = 0 \,, \qquad (3)$$

where μ is the magnetic permeability, $\boldsymbol{H_c}$ is the coercive magnetic field of permanent magnets, $\boldsymbol{J}$ is the current density flowing through the stator coils (a priori unknown).

In order to solve (3), circuit models are associated to the electromagnetic field models of the machines.

Dirichlet boundary conditions ($\boldsymbol{A} = 0$) are imposed on the outer and inner boundaries of the FEM computation domain.

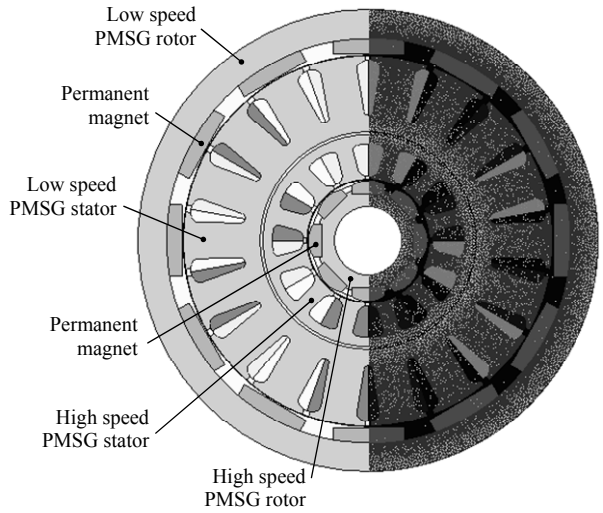

Fig. 2 – FEM 2D computation domain and mesh.

By solving (3) the chart of the magnetic flux density of the two coaxially embedded PMSGs in no-load operation are obtained as shown in Fig. 3.

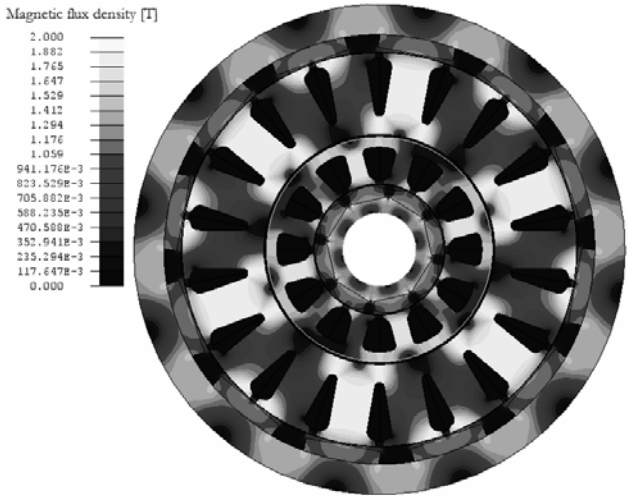

Fig. 3 – Main parts of the studied PMSG (cross sectional area).

The main data obtained by analytical and FEM calculations for the two coaxially embedded PMSGs are shown in Tables 1 and 2. The FEM analysis allowed also determining the machine parameters that were extracted to be used in Matlab-Simulink simulations of the control system of the CRWS.

Table 1

Main data of the high speed PMSG

Rated power [VA]	400
Rated voltage [V]	150
Rated current [A]	1.54
Phase resistance [Ω]	7.04
L_d inductance [mH]	21.15
L_q inductance [mH]	29.52
Rated speed [rpm]	750
No. of pole pairs	4
Axial length [mm]	150
Stator bore diameter [mm]	44

Table 2

Main data of the low speed PMSG

Rated power [VA]	600
Rated voltage [V]	150
Rated current [A]	2.31
Phase resistance [Ω]	2.83
L_d inductance [mH]	5.08
L_q inductance [mH]	8.42
Rated speed [rpm]	600
No. of pole pairs	6
Axial length [mm]	50
Stator bore diameter [mm]	138

3. MATLAB-SIMULINK MODEL OF CRWS CONTROL SYSTEM

The numerical model of the CRWS control system is developed using Matlab-Simulink environment and it is decoupled from the analytical calculation and FE analysis of the two PMSGs.

The ac electrical energy produced by each of the two PMSGs is characterized by variable frequency and voltages, depending on the wind speed. That is why an ac to dc conversion module should be used in the first stage. Then, the obtained dc energy is converted back to ac at constant parameters imposed by the grid to which the CRWS is connected. This process is depicted in Fig. 4 using a general bloc diagram.

The wind turbines and PMSGs have been modeled using specific Simulink/PowerSystems blocks as shown in Fig. 5. The machines parameters were obtained previously by analytical and FEM calculations. The wind turbines have fixed blades so their pitch angles were set to zero degrees in the reference p.u. wind turbine model implemented in Matlab-Simulink environment. The turbine models used for computations The ac to dc conversion is ensured by two diode rectifiers (Fig. 7).

In order to extract the maximum power, the system must operate as close as possible to the peak point of the wind turbine power characteristics. This task is accomplished by a dc to dc converter (Fig. 8) controlled by a maximum power point tracking (MPPT) algorithm detailed in Fig. 6.

The maximum power points of the two turbines and correspond to certain generator speed values, were mapped for different wind speeds into specific lookup table blocks. A proportional integral (PI) controller

compares this "desired" value with the real generator speed and sends a command to the dc to dc converter in order to decrease this error. In this way the generator speed will change to reach the maximum power operation area. A dc to dc boost converter was chosen because the PMSG has a low output voltage.

The whole system is connected to a three phase power grid (0.4 kV, 50 Hz), using controlled inverters as in Fig. 9. The synchronization between each inverter and the power grid is assured by grid voltage measurement (Fig. 10).

The grid was modeled as a three phase ac source with a high power series RL load as in Fig. 11.

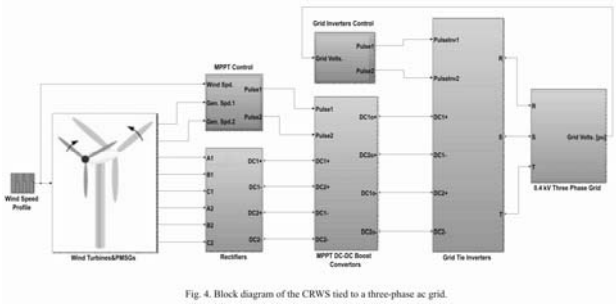

Fig. 4 – Block diagram of the CRWS tied to a three-phase ac grid.

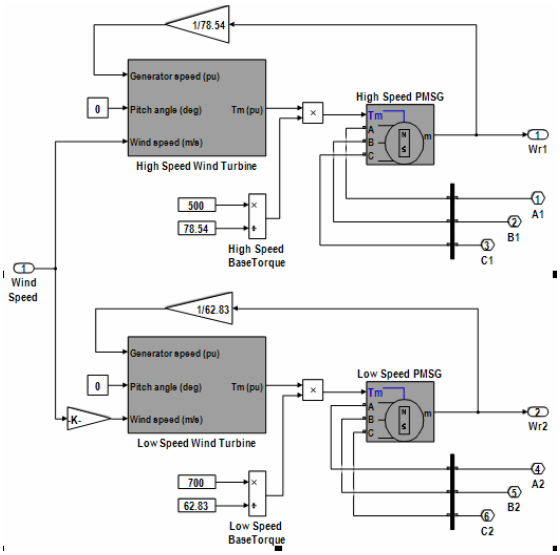

Fig. 5 – Details of wind turbines & PMSG block.

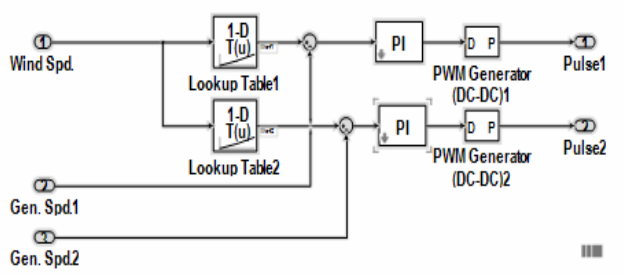

Fig. 6 – Details of MPPT control block.

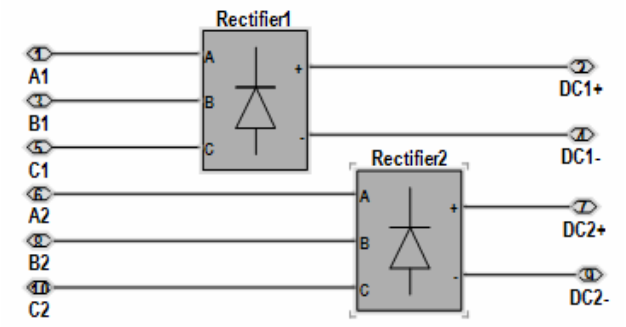

Fig. 7 – Details of rectifiers block.

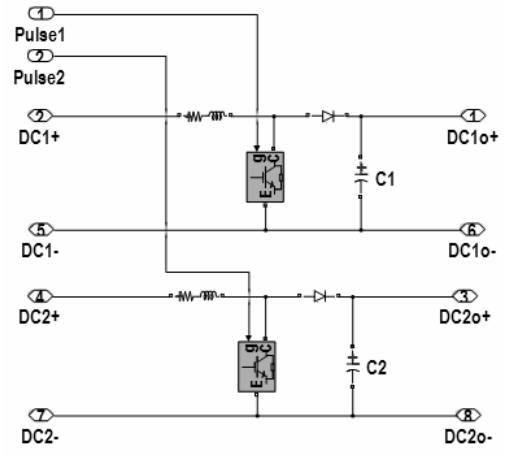

Fig. 8 – Details of MPPT dc-dc boost converters block.

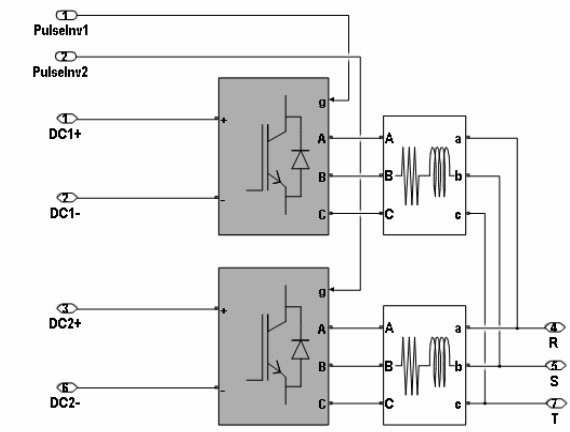

Fig. 9 – Details of grid tie inverters block.

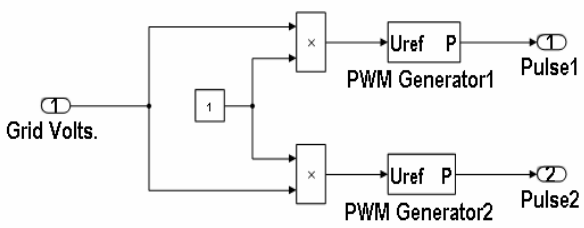

Fig. 10 – Details of grid inverters control block.

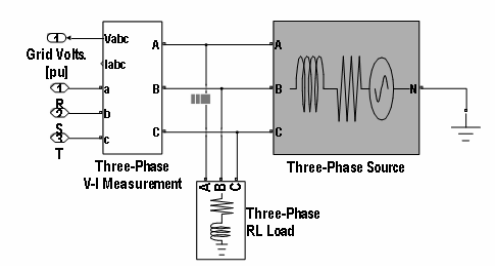

Fig. 11 – Details of 0.4 kV three phase grid block.

The PMSGs are permanent magnet synchronous machine blocks from Simulink library that operates as generators. Sinusoidal model was adopted, this assumes that the stator magnetic flux has a sinusoidal distribution and that the electromotive forces are also sinusoidal.

The PMSG equations (4) are expressed in the rotor reference frame (dq frame). All quantities in the rotor reference frame are referred to the stator [15].

$$\begin{aligned}\frac{\mathrm{d}}{\mathrm{d}t}i_d &= \frac{1}{L_d}v_d - \frac{R}{L_d}i_d + \frac{L_q}{L_d}p\omega_m i_q \\ \frac{\mathrm{d}}{\mathrm{d}t}i_q &= \frac{1}{L_q}v_q - \frac{R}{L_q}i_q - \frac{L_d}{L_q}p\omega_m i_d - \frac{\lambda p\omega_m}{L_q}, \\ T_e &= 1.5p\left[\lambda i_q + (L_d - L_q)i_d i_q\right]\end{aligned} \quad (4)$$

where:

L_d, L_q – d and q axis inductances,
R – resistance of the stator winding
i_q, i_d – q and d axis currents
v_q, v_d – q and d axis voltages
ω_m – angular velocity of the rotor
λ – amplitude of the flux produced by the permanent magnets in the stator phases
p – number of pole pairs
T_e – electromagnetic torque.

4. NUMERICAL RESULTS

The proper operation of the control system of the CRWS was tested by analyzing its response to a wind speed profile described by a step-like function shown in Figs. 12 and 14.

The control systems response in terms of output electric power at dc busbar level is shown in Fig. 12 for the high speed wind turbine and in Fig. 14 for the low wind speed turbine. The output power expressed in p.u. for each turbine and for each wind speed level is added on the corresponding wind turbine characteristics as shown in Figs. 13 and 15 respectively.

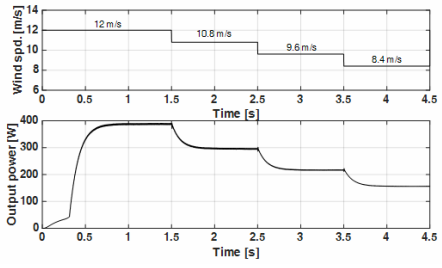

Fig. 12 – Response of high speed wind turbine.

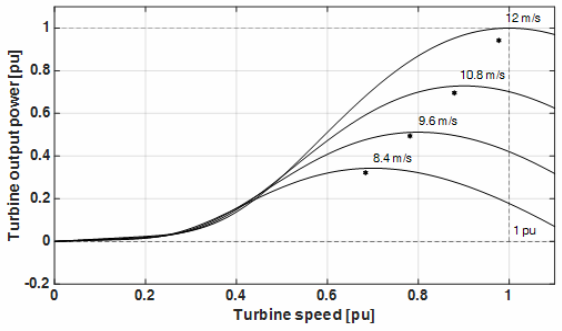

Fig. 13 – Power characteristics of high speed wind turbine.

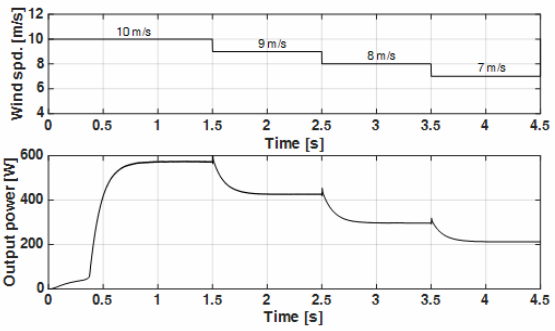

Fig. 14 – Response of low speed wind turbine.

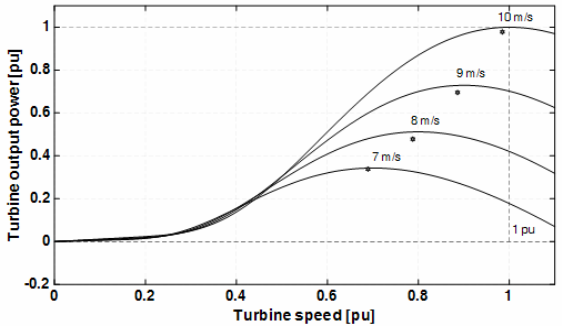

Fig. 15 – Power characteristics of low speed wind turbine.

The numerical results show that both counter rotating wind turbines operate in the maximum power range and the control systems are well adjusted providing high performance results. The obtained electric powers are slightly smaller than the maximum ones manly due to the losses dissipated in the PMSGs and rectifiers.

5. CONCLUSIONS

This paper deals with the numerical analysis of a small power grid tie CRWS. The electric drive proposed in the paper, based on an electro-mechanical converter with two coaxially embedded PMSGs, is an original, reliable and compact brushless solution, different from the existing ones, detailed in [11] and [12].

The design of the machine was based on analytical calculation as well as on FEM analysis (Flux ® software package). The parameters of the PMSGs were extracted from electromagnetic field solution and inserted into the control system of the CRWS whose operation was simulated using Matlab/Simulink development environment.

The operation of the control system of the CRWS was analyzed in various wind conditions and the numerical results proved a proper response and a reliable design.

ACKNOWLEDGEMENTS

This paper was partly supported by the Bridge Grant Programme – PNCDI III, financed by UEFISCDI, project no. 68BG/2016.

Received on March 22, 2018

REFERENCES

1. ***, *Wind in power – 2016 European statistics*, Wind Europe, 2017 (windeurope.org).
2. S. Tamalouzt, K. Idjdarene, T. Rekioua, R. Abdessemed, *Direct Torque Control of Wind Turbine Driven Doubly Fed Induction Generator*, Rev. Roum. Sci. Techn. – Électrotechn. et Énerg., **61**, *3*, pp. 244–249 (2016).
3. O. Aouchenni, R. Babouri, K. Ghedamsi, D. Aouzellag, *Wind Farm Based on Doubly Fed Induction Generator Entirely Interfaced with Power Grid Through Multilevel Inverter*, Rev. Roum. Sci. Techn. – Électrotechn. et Énerg., **62**, *2*, pp. 170–174 (2017).
4. L. Barote, C. Marinescu, *Modeling and Operational Testing of an Isolated Variable Speed PMSG Wind Turbine with Battery Energy Storage*, Advances in Electrical and Computer Engineering Journal, **12**, *2*, pp. 81–88 (2012).
5. N.S. Patil, Y.N. Bhosle, *A review on wind turbine generator topologies*, Proc. of International Conference on Power, Energy and Control (ICPEC), India, 2013.
6. K. Ahsanullah, R. Dutta, M.F. Rahman, *Review of PM generator designs for direct-drive wind turbines*, Proc. of 22nd Australasian Universities Power Engineering Conference (AUPEC), Indonesia, 2012.
7. L.L. Amuhaya, M. J. Kamper, *Design by optimisation of a buried PM variable-flux wind generator for grid connection*, Proc. of International Conference on Optimization of Electrical and Electronic Equipment (OPTIM) & 2017 International Aegean Conference on Electrical Machines and Power Electronics (ACEMP), Romania, 2017.
8. P. C. Sai, S. Richa, R. Yadav, R. Nihar Raj, G. R. K. Gupta, *Design and simulation of high efficiency counter-rotating Vertical Axis Wind Turbine arrays*, Proc. of Int. Conference and Utility Exhibition on Green Energy for Sustainable Development (ICUE), 2014, pp. 1–9.
9. M. Agung Bramantya, Luqman Al Huda, *An experimental study on the mechanics power of counter rotating wind turbines model related with axial distance between two rotors*, Proc. of the Int. Annual Engineering Seminar (InAES), 2016, pp. 212–217.
10. Yosua Heru Irawan, M. Agung Bramantya, *Numerical simulation of the effect of axial distance between two rotors in counter-rotating wind turbines*, in Proc. of the International Conference on Science and Technology-Computer (ICST), 2016, pp. 1–5.
11. M. Popescu, G. Oprina, A. Mitulet, S. Nicolaie, R. Chihaia, A. Nedelcu *et al*., *Aspects regarding the application of electric generators to wind energy conversion using counter rotating turbines*, Proc. of the IEEE International Symposium on Advanced Topics in Electrical Engineering (ATEE), 2013, pp. 1–4.
12. L. Melcescu, T. Tudorache, O. Craiu, M. Popescu, *Finite element analysis of a wind generator with two counter-rotating rotors*, Proc. of International Conference on Optimization of Electrical and Electronic Equipment (OPTIM) & 2017 International Aegean Conference on Electrical Machines and Power Electronics (ACEMP), Romania, 2017.
13. ***Cedrat: *User guide Flux® 11*, 2015.
14. I. Cioc, C. Nica, *Design of Electrical Machines* (in Romanian), Edit. Didactică și Pedagogică, Bucharest, 1994.
15. *** Matlab documentation, *www.mathworks.com/help/physmod/sps/powersys/ref/permanentmagnetsynchronousmachine.html*